Capability of the Complex EOF analysis : with demonstrations to the NCEP data

Ichikawa, Kaoru
Research Institute for Applied Mechanics

Suito, Keiko
World School Nework | Department of Earth System Science and Technology, Interdisciplinary Graduate School of Engineering Sciences, Kyushu University

https://doi.org/10.15017/16655

出版情報：九州大学大学院総合理工学報告. 24 (1), pp.23-28, 2002-06. 九州大学大学院総合理工学府
バージョン：
権利関係：

九州大学大学院総合理工学報告
第24巻 第1号23-28頁 平成14年6月

Engineering Sciences Reports, Kyushu University
(KYUSHU DAIGAKU SOGORIKOGAKU HOKOKU)
Vol. 24, No. 1 pp. 23-28 JUNE 2002

Capability of the Complex EOF analysis — with demonstrations to the NCEP data

Kaoru ICHIKAWA*1*2,† and Keiko SUITO*3*4

†E-mail of corresponding author: *ichikawa@riam.kyushu-u.ac.jp*

(Received March 30, 2002)

The capability of the complex empirical orthogonal function (CEOF) analysis is first examined by applying it to ideal artificial test data. Then, real observations, or the NCEP surface temperature data, are analyzed by the CEOF method in order to understand practical skills and limitations of the CEOF analysis to describe actual oceanic variations.

Key words : *Complex EOF analysis, empirical orthogonal modes, sea surface temperature, NCEP data*

1. Introduction

Oceanographic phenomena consist of various scales in both space and time. Observations of these phenomena are thus very complicated, so that an analysis is desirable which can decompose the data into independent modes. The empirical orthogonal function (EOF) analysis, therefore, has been widely used in descriptive oceanography and meteorology.[1-4] Also, its extension, or the complex EOF (CEOF) analysis, which can treat phase-propagating modes is recognized as a very powerful tool.[5-10]

However, both the EOF and CEOF analyses are based only on statistical relationship among data points, thus their results are generally difficult in physical interpretation. Furthermore, restrictions of the analysis may cause unrealistic decomposition of a single simple phenomenon. These problems would be especially severe when temporal and spatial structures of each single mode are discussed in order to find physical causes of the modes.

Therefore, in the present paper, capability of the CEOF analysis is considered by applying the analysis to ideal artificial test data. The results of these performance tests of the CEOF analysis will be summarized in Section 2, followed by Section 3 describing demonstrative examples applying the CEOF analysis to the real NCEP surface temperature data. The discussions and concluding remarks will be provided in Section 4.

*1 Department of Earth System Science and Technology
*2 also, Research Institute for Applied Mechanics
*3 Department of Earth System Science and Technology, Graduate student
*4 Current affiliation: World School Network

2. Performance tests

2.1 Configuration

In the EOF analysis, any signal $y(\boldsymbol{x},t)$ will be decomposed by combination of N modes, assuming functional separation of variables; namely,

$$y(\boldsymbol{x},t) = \sum_{j=1}^{N} S_j(\boldsymbol{x})\, T_j(t). \tag{1}$$

Meanwhile, the CEOF analysis is an extension of EOF analysis in the complex numbers so that it allows a concept of phase and amplitude;[5-8,10] namely,

$$y(\boldsymbol{x},t) = \sum_{j=1}^{N} Re\left\{ S'_j(\boldsymbol{x})\, e^{i\phi_j(\boldsymbol{x})}\ T'_j(t)\, e^{-i\psi_j(t)} \right\}. \tag{2}$$

In the CEOF analysis, therefore, phase propagation can be treated by a term $\phi_j(\boldsymbol{x}) - \psi_j(t)$.

In the following tests, time series of one-dimensional variations $y(x,t)$ are first created for 51 points (x=1~51) for 51-time observations (t=1~51). Then these artificial input data are decomposed by the CEOF (and EOF) analysis, and capability of the analysis is considered by comparing reconstructed signal of each mode with the original input data.

2.2 Simple Propagating Waves

To study most simple case, propagating sinusoidal waves are first considered as

$$y(x,t) = A\sin(kx - \omega t), \tag{3}$$

with $k = 2\pi/10.2$ and $\omega = 2\pi/10.2$ (hereinafter, Case A).

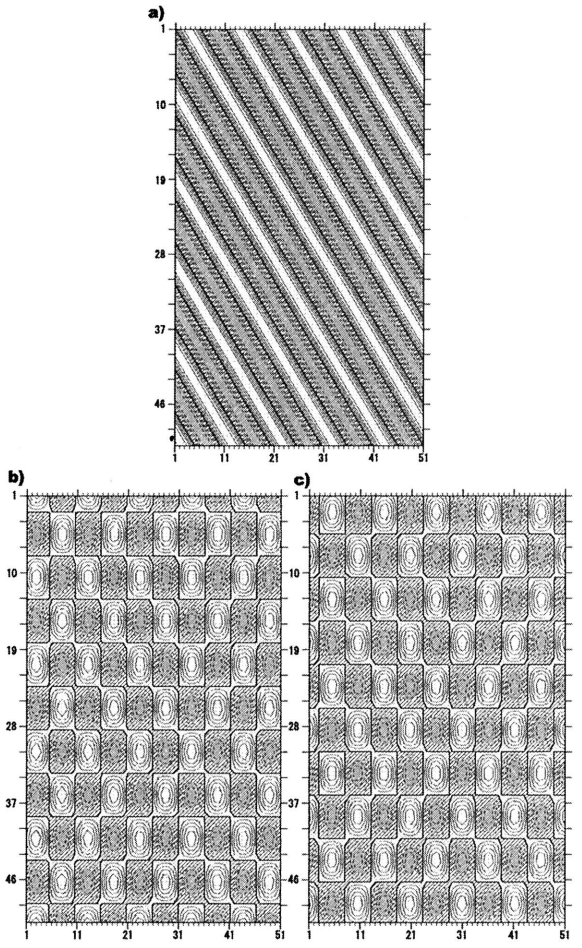

Fig. 1 Reconstructed signal $y(x,t)$ for the first CEOF mode (a), and the first (b) and the second (c) EOF modes of Case A, plotted as x in the horizontal axis and t in the vertical axis. The contour interval is $0.2A$ and negative values are shaded heavily. The contribution ratios are 100% for **a**, 50% each for **b** and **c**.

As expected from Eq. (2), the CEOF can treat these signals as a single mode (Fig. 1a). On the contrary, since the EOF modes should be consistent with the assumption of functional separation of variables, the EOF analysis further decomposes the signal y into two modes (Figs. 1b, c), following the reformation of Eq. (3) as

$$y(x,t) = A\sin kx\cos\omega t - A\cos kx\sin\omega t. \quad (4)$$

Therefore, if the data to be analyzed are known to be dominated by phase propagating phenomena, there would be no meaning in interpreting each single EOF mode independently.

2.3 Modified Propagating Waves

In this subsection, tests are expanded to take account of spatial variations of the amplitude A and

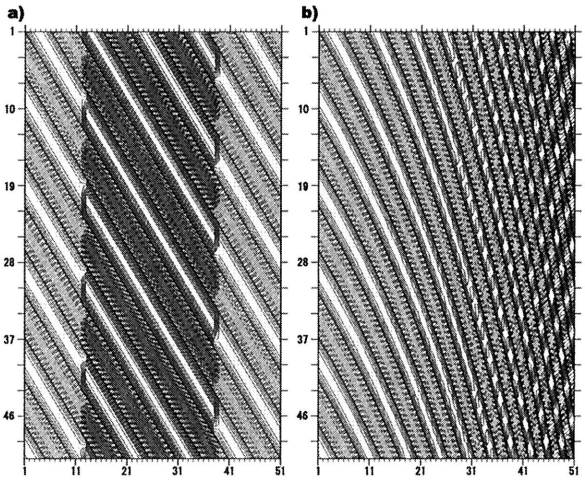

Fig. 2 The first CEOF modes for Case B1 (a) and B2 (b). The contour interval and shadings are same as Fig. 1. The contribution ratios are both 100% for **a** and **b**.

the wavenumber k. In Case B1, spatially amplified propagating waves are examined; namely,

$$y(x,t) = A(x)\sin(kx - \omega t), \quad (5)$$

where

$$A(x) = \begin{cases} A & \text{(both sides)} \\ 2A & \text{(center).} \end{cases}$$

The parameters k and ω are set as the same as Case A. Meanwhile, wavenumbers varying linearly in space are considered in Case B2; namely,

$$y(x,t) = A\sin\left(k(x)x - \omega t\right), \quad (6)$$

where

$$k(x) = k_s + \frac{k_e - k_s}{X_e - X_s}(x - X_s).$$

In the test, k_s is set as $2\pi/10.2$, $k_e = 2\pi/5.2$, $X_s = 0$, $X_e = 51$, and $\omega = 2\pi/10.2$.

As shown in Fig. 2, both signals are treated as a single CEOF mode. Similarly to these, waves with amplitudes and frequencies changing in time, or $A(t)$ and $\omega(t)$, are also handled well in the CEOF analysis.

2.4 Sinusoidal waves with $k(t)$ or $\omega(x)$

On the contrary to Case B2, waves with wavenumbers changing in time, $k(t)$, or those with frequencies varying in space, $\omega(x)$, are unable to be handled in a single CEOF mode. As shown in Eq. (2), variables x and t should independently contribute to the phase of a CEOF mode, so that

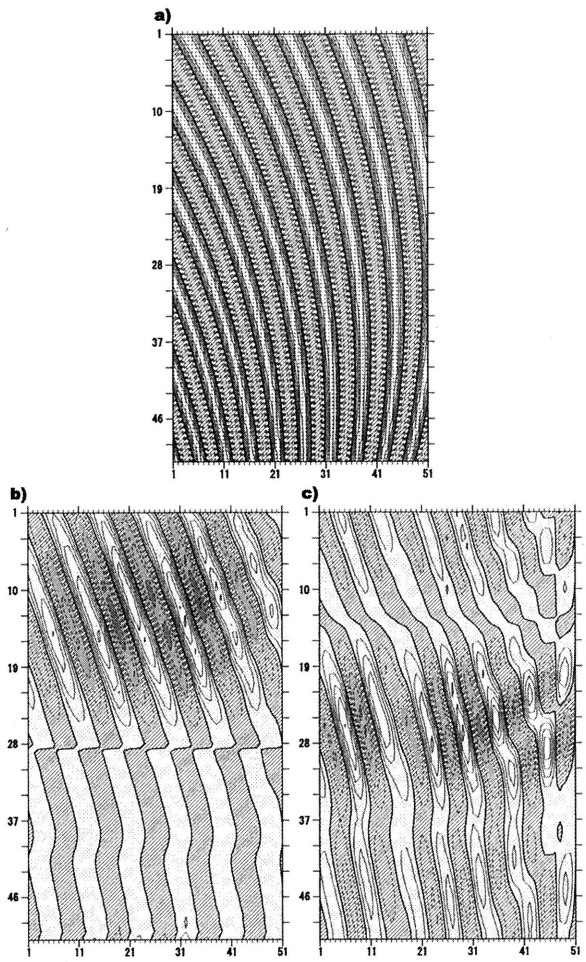

Fig. 3 The original signal of Case C (a) and the first (b) and second (c) CEOF modes. The contour interval and shadings are same as Fig. 1. The contribution ratios are 31% for **a** and 24% for **b**.

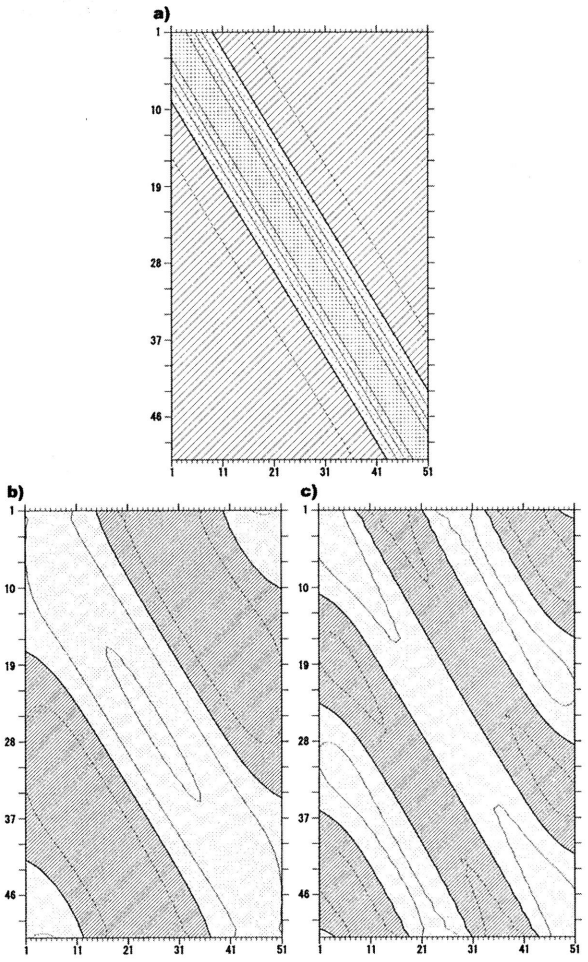

Fig. 4 The original signal of Case D (a) and the first (b) and second (c) CEOF modes. The contour interval and shadings are same as Fig. 1. The contribution ratios are 62% for **a** and 28% for **b**.

the CEOF mode cannot express phase propagations depending on both t and x, such as $k(t)x$ or $\omega(x)t$.

Case C is a test for waves with the wavenumbers varying linearly in time; namely,

$$y(x,t) = A\sin\left(k(t)x - \omega t\right) \tag{7}$$

with

$$k(t) = k_s + \frac{k_e - k_s}{T_e - T_s}(t - T_s). \tag{8}$$

In the test, $T_s = 0$, $T_e = 51$, and the other parameters k_s, k_e and ω are set as the same as Case B2.

The first two CEOF modes are plotted in Fig. 3. Note that the accumulated contribution ratio of the two modes accounts only 55% of the total variance so that more modes are necessary to reconstruct the whole signal. Both the first (Fig. 3a) and the second (Fig. 3b) modes behave as propagating waves with fixed wavenumbers whose amplitude changes in time. The wavenumber of the first mode is similar to k_s and the amplitude is significant only in the earlier t period (*e.g.* $t < 22$). On the other hand, the former of the second mode is somewhat closer to $(k_s + k_e)/2$, and the middle t (*e.g.* $19 < t < 33$) is the period of stronger amplitude.

Therefore, several CEOF modes are necessary to be accumulated to treat those waves with temporal modulation of wavenumbers. This kind of situation may occur in the real ocean when waves are generated by responding to some constant forcing (say, tides or annual wind stress variations) but their phase speeds are varying in time by changes in vertical density structures of the ocean. In such cases, each CEOF mode may correspond to waves at a certain density structure.

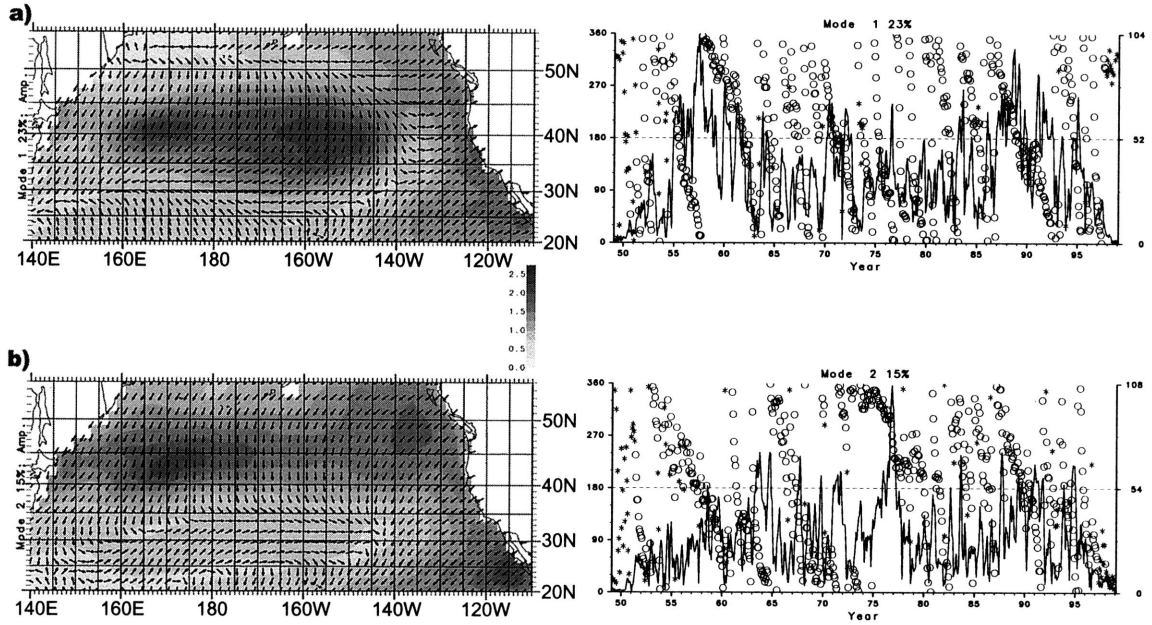

Fig. 5 The first (a) and second (b) CEOF modes for the monthly NCEP surface temperature anomaly. The amplitude and phase distribution in space (S'_j and ϕ_j) are shown in the left panel, and these for the temporal changes (T'_j and ψ_j) in the right panel (b). In the left panel, the phase at each point is shown by the direction of an arrow, and an area of larger amplitude is shaded more heavily. In the right panel, the phase change is shown by open circles with left axis in degree unit, and the amplitude is indicated by a thin line with right axis in arbitrary unit. The contribution ratios for the first and the second modes are 23% and 15%, respectively.

2.5 Propagating Packet

For the last test, a propagating packet is to be considered. A Gaussian packet is introduced here as

$$y(x,t) = A\exp\left(-\left(\frac{x-ct}{X_L}\right)^2\right) - \bar{y}, \qquad (9)$$

where

$$\bar{y} = \frac{\iint y(x,t)dxdt}{\iint dxdt}, \qquad c = \frac{\omega}{k}.$$

In Case D, k and ω are set as the same as Case A and $X_L = 6.375$ is selected.

Since relative phase difference between any two points changes greatly in time in Case D, separation of the CEOF modes would occur as seen in the previous subsection. Spatial and temporal characteristics of the CEOF modes of Case D are, however, very different from these of Case C. As shown in Fig. 4, all these CEOF modes of Case D are recognized as propagating waves with different wavenumbers but the same phase speed c. Therefore in this case, not only the original packet signal is separated into several CEOF modes, but also physical interpretation of each single CEOF mode would be depart from that of the original signal.

3. Application to the NCEP data

In addition to these ideal tests, the CEOF analysis is further applied in the present paper to real observational data in order to understand its practical skills. We here used 50 years of monthly National Center for Environmental Prediction (NCEP) reanalysis surface temperature data starting from 1949.[3,11] The study area is selected for 140°E–110°W and 20°N–55°N on an almost 2° grid. At each grid point, the mean and a long-term linear trend are first removed, and then the CEOF analysis is applied.

The results for the first CEOF mode are shown in Fig. 5a. From the left panel of the figure, the variations in this mode are amplified at the center of the study area at around 40°N, and along the eastern coastal boundary. The phases of those two areas are almost opposite, so that the temperature of the two areas would seesaw with a node at about 145°W.

From the right panel of Fig. 5a, the frequency of this mode is found variable. Although the dominant frequency seems to be annual, interannual frequencies clearly override the annual one during periods around 1960 and 1990.

Meanwhile, the amplified areas for the second

CEOF mode are bounded in a band between 40°N and 50°N (Fig. 5b; left panel). Note that there is no significant phase variation within those areas, so that the spatial scale of the second CEOF mode is large in the longitudinal direction. It should also be noted that these areas are somewhat close to the northern edge of that of the first mode at 40°N (Fig. 5a; left panel).

Similarly to the first mode, frequency of the second mode is also a mixture of annual and interannual ones. In the period when interannual frequency dominates the first mode variation (say, late 1950's), however, phase variation of the second mode seems to be slower than that of the first mode. Taking into account of the larger spatial scales of the second mode, phase speeds of two modes become similar in some areas around 40°N.

Considering the results of Case D, the similarity of phase speed with different spatial scales may be caused by separation of a single propagating packet. In order to examine this possibility, the temperature anomaly field is reconstructed for the first mode alone and for the accumulation of the two modes (Fig. 6). The left and right panels show almost similar temperature pattern until March, 1958 (Fig. 6c). Then the combined modes show clear eastward propagation of a packet with decreasing its amplitude, while the single first mode shows almost no propagation in 1958–1959. The speed of the eastward propagation in the right panels is determined as 1–2 cm/s, which seems too slow for any atmospheric signal. Since the eastward Kuroshio Extension exists in this area at around 40°N, advection by oceanographic currents is consistent with the eastward speed of 1–2 cm/s. Note again that the eastward advection is not found in the CEOF mode alone.

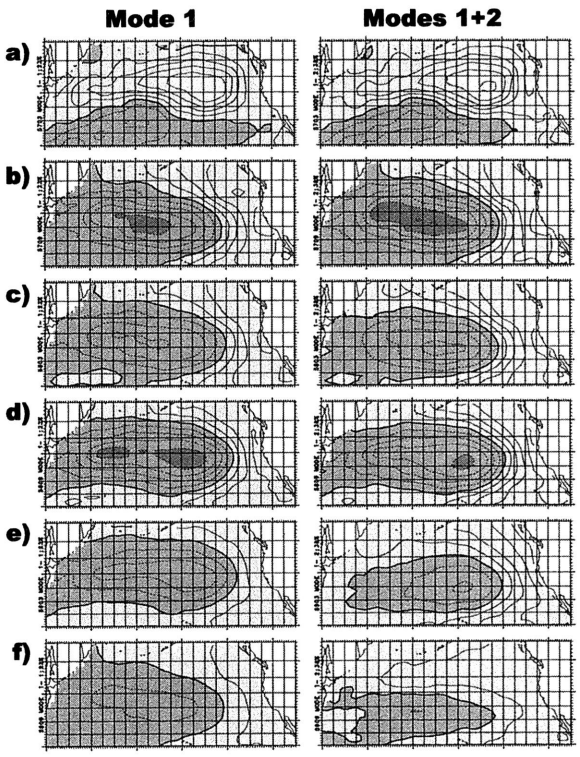

Fig. 6 Reconstructed temperature anomaly field for the CEOF 1st mode (left) and for the accumulated 1st and 2nd modes (right) in March 1957 (a), September 1957 (b), March 1958 (c), September 1958 (d), March 1959 (e), and September 1959 (f). The contour interval is 0.25°K and areas of lower temperature anomaly are shaded heavily.

4. Summary

The capability of the CEOF analysis is first examined by ideal artificial input data. As expected from Eq. (2), the CEOF analysis handles very well for Cases A and B, which examine propagating waves with spatially varying amplitude and wavenumber, or those with temporally changing amplitude and frequency. However, when variables $\boldsymbol{x}$ and t are not independent to the amplitude and phase variations, the signals are treated in separate CEOF modes (Cases C and D). Especially, when phase propagating packets are analyzed, they are separated into several CEOF modes, each of which behaves as propagating waves with different wavenumbers but with the same phase speed. These modes are physically consistent with the original signals only when they are accumulated.

The case with phase propagating packets may be actually found in the analysis of real data. The NCEP surface temperature anomaly data are analyzed by the CEOF method, and the results indicate that a packet slowly advected eastward is decomposed separately into the first and the second CEOF modes. Since the advection speed is somewhat consistent with the existence of the Kuroshio Extension at around 40°N, accumulation of the two modes seems to be essential as in Case D during late 1950's when the phase speeds of the two modes are similar to each other.

In Case D, however, the results would be approximately close to the simple propagating waves when the spatial scale X_L is much larger than the size of the study area. In other words, the capability of the CEOF analysis would depend on the choice of the area and the period to analyze. It would be therefore important to check consistency

of the results by altering size of the area or duration of the period.

Acknowledgments

We would like to thank Dr. Takashi Setou for his helpful commitment in our discussions. Prof. Shiro Imawaki also gave us valuable suggestions on interpretation of the results.

References

1) Weare, B.C., A. Navato and R.E. Newell, *J. Phys. Oceanogr.*, 6, 671–678 (1976).

2) Overland, J.E. and R.W. Preisendorfer, *Mon. Weath. Rev.*, 110, 1–4 (1982).

3) Nakamura, H., G. Lin and T. Yamagata, *J. Meteor. Soc. Japn.*, 2215–2225 (1997).

4) Tanimoto, Y., N. Iwasaka, K. Hanawa and Y. Toba, *J. Climate*, 6, 1153–1160 (1993).

5) Barnet, T.P., *Mon. Wea. Rev.*, 111, 756–773 (1983).

6) Horel, J.D., *J. Clim. Appl. Met.*, 23, 1660–1673 (1984).

7) White, W.B., S.E. Pazan and M. Inoue, *J. Phys. Oceanogr.*, 17, 264–280 (1987).

8) Merrifield, M.A. and R.T. Guza, *J. Phys. Oceanogr.*, 20, 1628–1633 (1990).

9) Ichikawa, K. and A. Kaneda, *La Mer*, 38(4), 219-226 (2000).

10) Ichikawa, K., *J. Oceanogr.*, 57(1), 55–68 (2001).

11) Kalnay, E., M. Kanamitsu, R. Kistler, W. Collins, D. Deaven, L. Gandin, M. Iredell, S. Saha, G. White, J. Woollen, Y. Zhu, A. Leetmaa, R. Reynolds, M. Chelliah, W. Ebisuzaki, W.Higgins, J. Janowiak, K.C. Mo, C. Ropelewski, J. Wang, R. Jenne and D. Joseph, *Bul. Am. Met. Soc.*, 437–471 (1996).